Available online at www.sciencedirect.com
SCIENCE DIRECT®
Carbon 43 (2005) 986–993
CARBON
www.elsevier.com/locate/carbon

Solutal Bénard–Marangoni instability as a growth mechanism for single-walled carbon nanotubes

Frédéric Larouche *, Olivier Smiljanic, Xueliang Sun, Barry L. Stansfield

INRS-Énergie, Matériaux et Télécommunication, Université du Québec, 1650 Boulevard Lionel-Boulet, Varennes, Québec, Canada J3X 1S2

Received 3 March 2004; accepted 17 November 2004

Abstract

In the past few years, considerable progress has been achieved in understanding the growth mechanism of single-walled carbon nanotubes (C-SWNTs). Nevertheless, the nucleation of C-SWNTs still remains partially unexplained by these models. A study of the critical synthesis parameters in the plasma torch process and a review of existing growth mechanisms lead us to propose a new growth mechanism for bundles of C-SWNTs, based on the Bénard–Marangoni instability. It is shown that the conditions occurring at the surface of the catalyst nanoparticle (NP) during the growth of the C-SWNTs give rise to the solutal BMI, which in turn results in a pattern of hexagonal convection cells in the liquid layer on the surface of the NP. The vortex ring flow pattern within these cells is then responsible for the structured growth of the C-SWNT bundles. This model highlights the important parameters required to optimize the synthesis of C-SWNTs.

Keywords: Carbon nanotubes; Catalyst; Transmission electron microscopy; Interfacial properties

1. Introduction

Since 1993, there has been significant interest in the synthesis of single-walled carbon nanotubes (C-SWNTs) because of their exceptional properties [1,2]. However, the present low level of production slows down the commercial development of applications using this material. The present level of production of a few grams per day remains far from any commercial objective. The best way to optimize the production of C-SWNTs is via a thorough understanding of the growth mechanism. Much progress has been made in this direction in the last few years, but there are still aspects which need to be addressed. A better model of C-SWNT growth would allow us to better optimize the growth conditions and eventually to control the synthesis. Several techniques for the synthesis of C-SWNTs have been developed over the past few years. The most promising are still those which use a gas-phase method, such as the arc discharge [3,4], laser ablation [5,6], solar furnace [7,8], HiPco [9], as well as plasma torch [10]. These techniques produce in situ the precursors for the C-SWNT growth during the gas quenching, i.e. carbon and catalyst nanoparticles (NPs). In contrast, in CVD methods, catalyst NPs are generally deposited on a substrate and the carbon is obtained from the dissociation of a carbon-containing gas. They give, to our knowledge, exclusively isolated C-SWNTs (one C-SWNT per NP) or multi-walled carbon nanotubes (C-MWNTs). In the gas-phase methods, C-SWNTs can be found in two forms in the deposits, depending on the size of the NPs of the catalyst. The C-SWNTs will be isolated when the NP is of the same size as the diameter of the C-SWNT (0.7–3 nm). In most cases, however, C-SWNTs are found in the form of bundles of 10–100 individual nanotubes. The diameter of

* Corresponding author. Tel.: +1 450 929 8158; fax: +1 450 929 8102.
E-mail address: larouche@emt.inrs.ca (F. Larouche).

0008-6223/$ - see front matter © 2004 Elsevier Ltd. All rights reserved.
doi:10.1016/j.carbon.2004.11.029

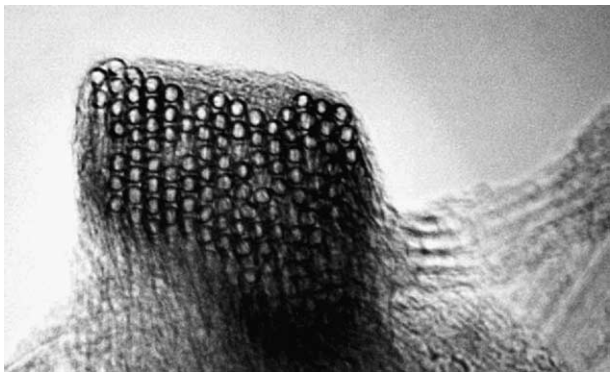

Fig. 1. Transverse view of a bundle of nanotubes showing the triangular lattice [6].

each C-SWNT is of the order of a nanometer, while the bundle has transverse dimensions of the order of 5–20 nm. While in some cases the bundles are seen to be the result of the coalescence of either single nanotubes or smaller bundles from different catalytic particles, many observations suggest that most bundles grow collectively from a single larger catalyst particle whose diameter is several nm [11].

Several models have been proposed to explain the growth of such bundles, but none has completely explained the nucleation of the C-SWNTs from the NPs even though they can well describe the general situation leading to the growth. The new model presented here applies principally to the growth of a bundle of C-SWNTs which emerges from the surface of a single catalyst NP and for which the C-SWNTs are organized in a triangular lattice [4,6] (see Fig. 1). This model is based on a surface tension driven instability [12–14], the solutal Bénard–Marangoni instability; it complements and extends existing models and provides an explanation for many experimental observations. The model highlights certain important parameters which are crucial for the production of C-SWNTs: the temperature range over which we must operate, and especially the non-equilibrium nature of the process, which is manifested by the observed importance of the cooling rate on the growth.

2. Present models describing the growth of C-SWNTs

The analysis of the present models [11,15–20] leads to a general scenario for the growth of C-SWNTs in the gas-phase techniques. The formation is seen to begin by the creation of hot vapor containing carbon and metal atoms in an inert gas. This mixture is initially at high temperature (~5000 °C) and contains an atomic fraction of about 3% metal catalyst with respect to carbon. This mixture is then cooled rapidly, at a rate of 10^5–10^6 K/s [20–22], to the synthesis temperature, which is typically around 1300 K, depending of the eutectic temperature of the carbon-catalyst binary system [7]. During this cooling phase, the vapor condenses to form NPs of carbon, as well as nanometer-scale droplets of metal–carbon solution. Spectroscopic measurements by Puretsky et al. [22] illustrate the temporal evolution of the process during laser ablation experiments: an initial formation of carbon NPs followed by those of metal and finally by the formation of the C-SWNTs.

The catalyst NPs, usually composed of transition metals (Fe, Co or Ni), are the key to the formation of the C-SWNTs in all gas-phase techniques; these NPs are produced during the rapid cooling process via the vapor phase condensation of metal atoms into droplets containing a large concentration of carbon because of the initial vapor composition. As these NPs cool, they will undergo a process of segregation wherein the surplus carbon is expelled radially towards the outside of the droplet, since the carbon is much less soluble in the solid phase than in the liquid and has a lower surface tension. Gavillet et al. [11] have shown that the carbon concentration in the catalyst NP after the growth of C-SWNTs is consistent with the segregation process. Combined with the integration of carbon from the surrounding vapor, this will result in a surface layer having a radial concentration gradient ($\nabla C = \Delta C/h$, see Fig. 2),

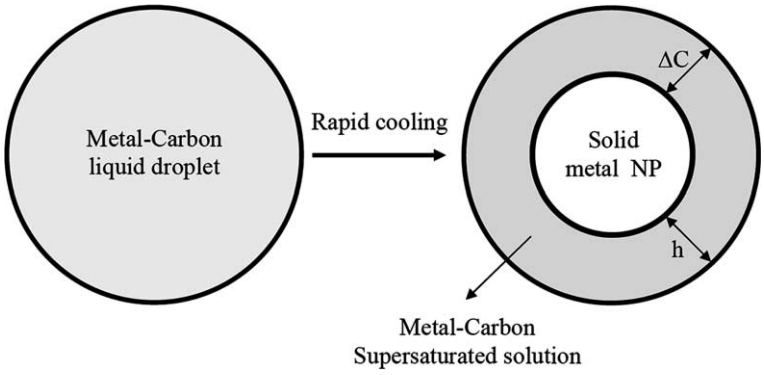

Fig. 2. Structure of the catalyst NP after the rapid segregation process and just before the nucleation of C-SWNTs, indicating the liquid layer of thickness h, in which there is a variation in concentration ΔC.

i.e. carbon will tend to accumulate toward the surface of the droplet. The concentration of carbon in the metal can attain a high value, up to 50% [23,24], which will greatly affect the structure of the catalyst NP and will maintain the existence of a liquid layer having a high degree of supersaturation. Jost et al. [18,19] have shown that the growth of the C-SWNTs is activated by a diffusion process with an activation energy characteristic of a liquid. This observation strongly suggests that a nanometer-scale liquid layer is present over the entire growth process.

A more complete overview of the growth mechanism of C-SWNTs can be obtained by combining the different observations and explanations of the present models. Hence, we can deduce that the role of the high cooling rate is, on one hand, to provoke the condensation of carbon NPs and nanometric metal–carbon droplets, the precursors for the synthesis of C-SWNTs. On the other hand, it ensures the formation of a layer with a high carbon concentration at the surface of the droplet. Indeed, the carbon accumulation in the surface layer, caused by the rapid segregation process [11], will maintain the existence of a liquid layer having a high degree of supersaturation while the core of the droplet would be transformed into a solid metal NP (see Fig. 2) since its carbon concentration is lower.

The presence of a liquid layer surrounding the solid metal NP can be explained by the fact that a solution containing a non-equilibrium carbon concentration (>25 at.% for Fe, Co, Ni) will have a melting temperature significantly lower than the eutectic point of the metal–carbon system at equilibrium [18,23]. It thus demonstrates a surface melting initiated by the weakening of the solid bonds caused by a very high concentration of inserted atoms, which results in a reduction of the surface enthalpy of melting [23]. Curvature can also cause a melting point reduction, but for the size of NPs considered here, it cannot explain a decrease in the melting point of more than a few hundred Kelvins. It is important to note that the liquid layer is far from thermodynamic equilibrium—it is in a state of supersaturation. Once the solid metal NP is formed, heterogeneous nucleation of carbon can take place at its surface, forming a bundle of C-SWNTs which grow simultaneously from their roots at the surface of the metallic NP, as proposed by Gavillet et al. [11].

The present models can well address the general situation leading to the formation of C-SWNTs, but they do not completely explain several aspects of the growth:

- The nucleation and the structure of C-SWNTs. Total energy calculations have shown that the formation of a cap or a capped nanotube is favored, but "kinetic factors" must be invoked to produce C-SWNTs having diameters of 1 nm [25].
- The collective organization of C-SWNTs into bundles exhibiting triangular lattice symmetry. These bundles are found to possess the same structure, independent of the synthesis technique and the nature of the catalyst. Although Van der Waals forces between tubes will tend to result in a "minimum energy" configuration having a triangular lattice [26], we must explain the observations which show that the triangular arrangement is imposed on the bundle right from its birth (see Fig. 12a in [11]). Moreover, the minimum energy consideration does not indicate how a network of C-SWNTs would sprout collectively from the solid metal NP.
- The range of temperatures over which the growth of the C-SWNTs takes place. It has been shown that synthesis occurs for temperatures slightly below the eutectic of the carbon–metal mixture [7,18], but physically it is less clear why there is a cut-off temperature at both higher and lower temperatures.
- The rapid growth of the C-SWNTs. The presence of diffusion in a liquid layer during the growth elucidates a part of this question, as discussed by Jost et al. [18], but their results suggest that the process is faster than pure diffusion.
- It has been suggested that instabilities at the surface of the NP could provide a necessary mechanism for the nucleation of nanotubes [11]. Indeed, the analogy with the Mullins–Sekerka instability, implied in dendritic growth of snow flakes, presents an interesting possible explanation of the nucleation of C-SWNTs [27]. However, the wavelength associated with this instability is incompatible with the size of C-SWNTs.
- The mechanism which determines the ability of a catalyst NP to nucleate a bundle of C-SWNTs instead of a C-MWNT.

3. Discussion

3.1. A re-examination of the role of the catalyst nanoparticles in the growth of C-SWNTs

The TEM image (Fig. 3) of a bundle of C-SWNTs produced via the plasma torch process permits us to see the small bundle emerging from the catalyst NP, each individual nanotube having a diameter close to 1 nm, also confirmed by Raman spectroscopy [21].

The transverse view of the bundle is known to possess a triangular lattice structure (Fig. 1). The morphology and the characteristics of the deposit produced by the plasma torch lead us to conclude that the growth mechanism is the same as that in the other gas-phase techniques [21]. In fact, for all these diverse techniques, Gavillet et al. [11] have already proposed that the growth mechanism is to be the same: an extended Vapor–Liquid–Solid model, the Root Growth Mechanism.

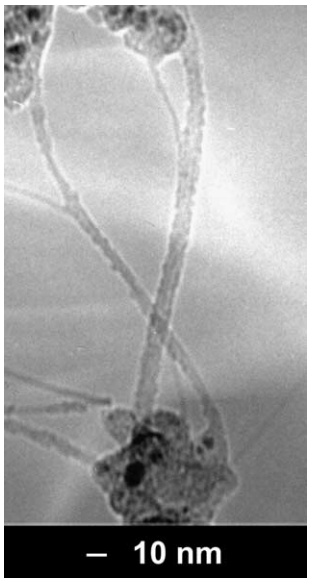

Fig. 3. TEM image of a small bundle of C-SWNTs that sprouts from a catalyst NP in the plasma torch process.

In the plasma torch process, we have found that the most important parameters to optimize the C-SWNT yield are the cooling rate, related to the thermal gradient, and the growth temperature [21]. The synthesis can be achieved for an oven temperature between 1000 and 1250 K, a temperature window slightly lower than the iron–carbon eutectic temperature; this observation is similar to what is observed in other processes [7,18,20]. The cooling rate is nevertheless the most sensitive parameter in the synthesis: it must be high enough to permit the formation of C-SWNTs. Similar results have been obtained recently in the arc-discharge technique [28]. We believe that the importance of the cooling rate on the C-SWNT yield is related to two different aspects: (1) the formation of the C-SWNT precursors and (2) the generation of a surface liquid layer on the catalyst NP. Indeed, the NP size distribution is crucial for the formation of the bundle of C-SWNTs. However, the cooling rate remains important even after the formation of the precursors [21], since the subsequent rapid cooling transforms the droplets into NPs having a solid metal core, surrounded by a liquid layer supersaturated in carbon (see Fig. 2). We are then obliged to analyze the consequences of having this surface liquid layer in the further solidification process of the catalyst NP.

3.2. The Marangoni effect in the catalyst liquid layer

The carbon concentration will have an important influence on the liquid properties, notably the surface tension: carbon acts like a surface-active solute. Transport of heat and mass in a thin liquid layer free to deform is dominated by the Marangoni effect, in contrast to the situation in thick liquid layers, where buoyancy is predominant. Indeed, we know from the literature [12,29] that the Marangoni effect is dominant in two general situations: in microgravity and in thin liquid layers, obviously the case for the nanometric liquid layer thickness, suspected in the growth of C-SWNTs. The Marangoni effect produces a mass transport along the liquid–gas interface resulting from the gradients of surface tension which are induced there. The gradients of surface tension can in turn be generated by inhomogeneities of temperature (the thermocapillary Marangoni effect) or impurity concentration (the solutal or diffusocapillary Marangoni effect) at the surface, since the surface tension depends on both of these. The solutal Marangoni effect is generally stronger than the thermocapillary effect because the surface tension is more sensitive to impurity concentration. The solutal Marangoni effect can even occur without any temperature inhomogeneities in the liquid layer [30]. As we have noted, rapid segregation of the carbon from the core is expected to result in a supersaturated liquid layer that is susceptible to significant inhomogeneities in the carbon concentration.

3.3. The Bénard–Marangoni instability and the growth of C-SWNTs

The conditions discussed above are such that we could expect the generation of the solutal Bénard–Marangoni instability (BMI) [12–14,29] within the liquid layer. The Marangoni number for the case of the solutal Marangoni effect can be estimated in a similar fashion to that for the case of thermocapillarity. Calculations show that for reasonable assumptions, the solutal Marangoni number Ma_s can exceed the value necessary for the generation of the BMI in contrast to the thermocapillary Marangoni number Ma_T which is very small ($Ma_T = 10^{-3}$). The surface tension of a metal–carbon solution varies between 0.8 and 2.1 N/m, depending of the carbon concentration [31]. It is known that the surface tension of a Fe–C solution increases linearly in the hypereutectic range when the concentration of carbon is increased, but no measurements are available for a 50%Fe–50%C solution. For the present calculation, we thus assume that the linear surface tension relation can be extrapolated to higher carbon concentration; we estimate the surface tension coefficient $\partial\sigma/\partial C$, obtained from the literature, to be 0.03 N/m per at.% of carbon [32]. As we have seen, segregation results in a radial carbon concentration profile through the liquid layer; we estimate the radial concentration difference ΔC to be 25% since the carbon concentration can vary from 25% to 50% from the bottom to the top of the liquid layer. The liquid thickness h is estimated to be about 3 nm from calculations based on carbon conservation during the segregation process and from the size of the catalyst NPs used in the synthesis of C-SWNTs.

The viscosity of the solution η is difficult to estimate, so we determine an upper limit by taking the viscosity value at the eutectic temperature and composition, which is 11.4 mPa s [31]. At higher carbon concentrations, intermolecular forces in the liquid will be weakened, resulting in a decrease of the viscosity. We assume that carbon diffusion in a highly supersaturated solution is equivalent to substitutional diffusion, which is almost independent of the nature of the solute in a liquid metal [33] and is of the order of 10^{-8}–10^{-9} m^2/s. In our calculation, we take the smaller value of 10^{-9} m^2/s for the carbon diffusion coefficient in the liquid metal D_{CL}, since the system is in a supersaturated state, which will tend to slow down the carbon diffusion because of the complete occupation of the solute sites. Using these values, we can determine the solutal Marangoni number Ma_s:

$$Ma_s = \frac{\frac{\partial\sigma}{\partial C}\Delta C h}{\eta D_{CL}} \approx 197$$

Ma_s is thus above the critical Marangoni number Ma^c ($Ma^c = 50$ for the insulating case [34]) for which the BMI will be generated according to the linear stability analysis. At the threshold of the instability, convection appears: a periodic pattern of hexagonal convection cells auto-organises in the fluid [12]: the Bénard–Marangoni cells. This pattern (see Fig. 4b) is a dissipative spatial structure characteristic of systems which are far from equilibrium [35]. These systems evolve from a disordered state to an ordered state as a result of fluctuations, i.e. inhomogeneities in surface tension in the present case. (Inhomogeneities in concentrations exhibiting a geometrical pattern (the Turing structure) or periodic variations of concentration (the Belousov–Zhabotinsky reaction) are other well-known examples [36] of dissipative structures.) We now analyse the effect of the convective pattern on the further carbon crystallization.

We see in Fig. 4a that each hexagonal convection cell in the pattern contains a vortex ring. The fluid rises from the center of the vortex ring, falling again at the edges of the hexagon cell, thus exhibiting a toroidal symmetry. From the top view (Fig. 4b), we note that the center of the vortex ring in each convection cell, where the fluid rises and which appears darker, are organized in a triangular lattice. The solutal BMI thus produces a pattern of convection cells with a characteristic wavelength λ_{BM}, which is known to be of the same order of magnitude as the thickness of the liquid layer h [12,37]; its magnitude is thus seen to be consistent with the diameter of the individual C-SWNTs since the vortex ring of inside diameter D_{VR} can be roughly estimated to be $\lambda_{BM}/2.5$ from Fig. 4b. The instability wavelength λ_{BM} or liquid thickness h required to obtain a vortex ring of inside diameter similar to the C-SWNT diameter is thus in the range of 2–8 nm. This is quite plausible if we consider that the size of the catalyst NPs which are observed to give rise to bundles of C-SWNTs varies generally from 5 to 20 nm [27].

We would thus propose an extended model to explain the nucleation and growth of bundles of C-SWNTs: the BMI model. In this model, we assume that the circulation of atomic C in the liquid layer (dissolved carbon) follows the flow pattern in the Bénard–Marangoni cells, like the aluminium particles in Fig. 4b. The carbon thus crystallizes within the center of the vortex ring at the solid–liquid interface, where heterogeneous nucleation can occur, as in the root growth mechanism proposed by Gavillet et al. From this nucleation site, the growing nanotube is carried upward by the flow of the convection cell. The growth of a bundle of C-SWNTs is thus the result of auto organization of carbon within a network of hexagonal convection cells generated by the BMI within a liquid layer surrounding a metal NP, as shown in Fig. 5a.

As was discussed previously, C-SWNTs are found isolated in CVD techniques and occasionally in gas-phase processes. In the present model, their growth can be seen as a borderline case, where the surface cannot support the convective pattern, but only a single convection cell because of its small size (Fig. 6). Actually, the C-SWNT diameter should be smaller than or

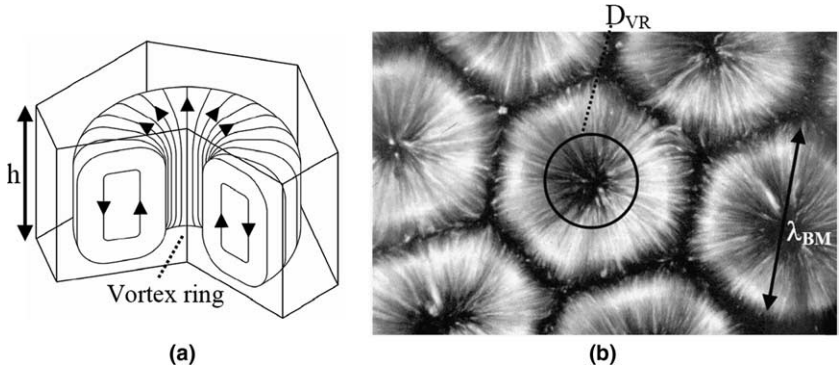

Fig. 4. (a) Front view of a hexagonal convection cell of depth h. (b) Top view of Bénard–Marangoni cells of wavelength λ_{BM} in silicon oil with aluminium particles [13], the picture is obtained by optical techniques.

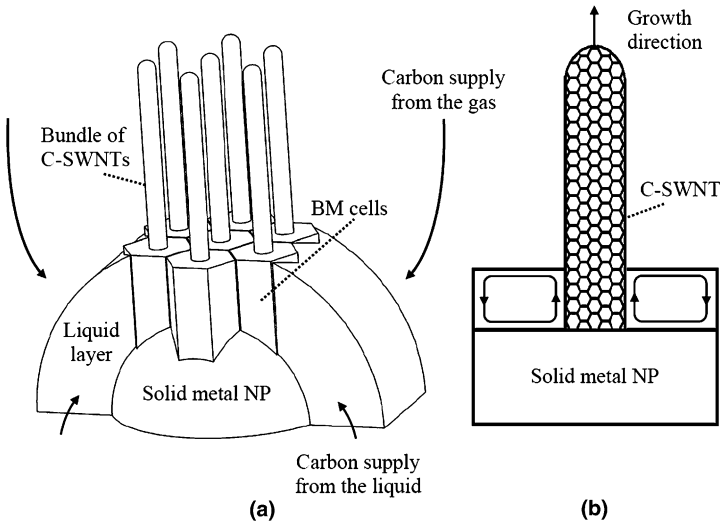

Fig. 5. The growth of a bundle of C-SWNTs based on the BMI. (a) Bundle growth in the pattern of convection cells. (b) Transverse view of the C-SWNT growth in an individual convection cell.

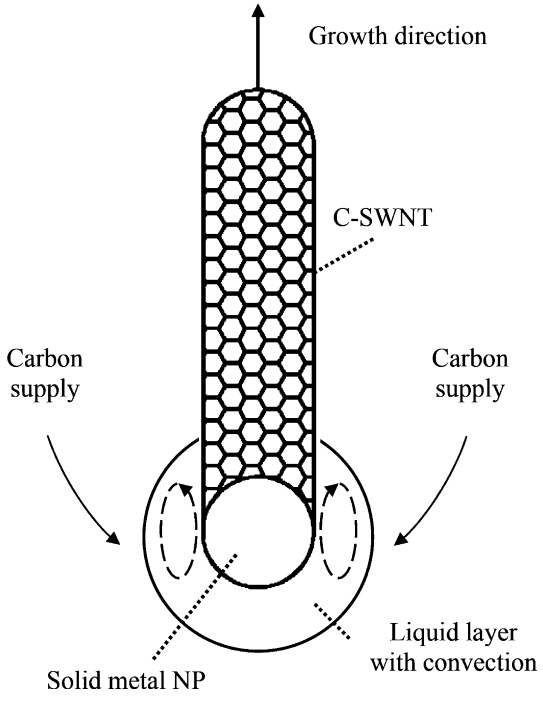

Fig. 6. The growth of an isolated C-SWNT on a solid metal NP.

equal to the catalyst NP size, since the diameter is correlated to the solid metal NP, which does not take into account the liquid layer thickness.

The presence of a liquid layer on the NP, necessary to generate the BMI, explains the temperature window within which the growth is possible. At low temperatures, the catalyst particle is completely solid, while at high temperature it becomes completely liquid. When the catalyst NP is completely liquid, there can no longer be carbon heterogeneous nucleation since the crystalline planes of the NP disappear.

The increase of the diameter of the C-SWNTs with the growth temperature is an experimental fact that has been noted by several authors [38,39]. In the BMI model, the diameter of the individual nanotubes is correlated to the size of the Bénard–Marangoni convection cells λ_{BM}, which changes when the thickness of the liquid layer is modified. When the temperature is above the eutectic temperature, all of the NP will be liquid, whereas at a low enough temperature it will be completely solid. It is thus logical to assume that the thickness of the surface liquid layer will increase monotonically with the growth temperature. Since we know from the literature that λ_{BM} increases with the liquid layer thickness h, we can qualitatively conclude that the diameter of C-SWNT will increase with the growth temperature.

The amount of carbon in the bundle of C-SWNTs exceeds significantly that present initially in the catalyst NP [11]; there must then be a contribution from the gaseous atmosphere. When the carbon from the liquid layer crystallizes, it liberates diffusion sites that can be filled by the carbon contained in the gas, which is absorbed at the surface of the liquid, and carried by the flow of the convection cells via a form of turbulent diffusion (convection) to the nucleation site of the bundle of C-SWNTs (see Fig. 5b). The BMI will thus substantially increase the rate of mass transfer at the liquid–gas interface, as well as in the liquid layer, because of the contribution from the Marangoni convection [40]. Consequently, the rapid rate of growth for C-SWNTs (~μm/s) certainly depends on the convection generated by the BMI. Jost et al. have obtained data which corroborate the presence of convection within the liquid layer [18]; which is consistent with the BMI mechanism proposed here.

The flows which are thought to be necessary for the growth of C-SWNTs are thus seen to be a natural result of the BMI. The "kinetic factors" which are deemed necessary for the formation of nanometer-scale tubes [25] are thus seen to be imposed by the structure of the Bénard–Marangoni convection cells. It could be expected that the flow in the center of the vortex ring is sheared; this would impress itself on the nucleating C-SWNT, suggesting that the origin of the C-SWNT chirality could be related to the flow structure in the convection cell. Moreover, the condition for the generation of the BMI, necessary for the C-SWNT nucleation, can explain why sulphur acts as a growth promoter, since it is a very efficient surface-active solute in a metal–carbon mixture [41].

4. Conclusion

The nucleation of bundles, which involves a collective growth of individual C-SWNTs, can now be seen as the result of the BMI in the liquid layer surrounding the solid metal NP, while the cylindrical structure of the C-SWNTs is caused by the crystallization of the carbon within the center of the vortex ring of the Bénard–Marangoni cells. Moreover, the organization of the C-SWNTs in the bundle into a triangular lattice is seen to be the natural result of the organization of the network of vortex rings in the Bénard–Marangoni cells (see Figs. 4b and 5a).

The generation of the BMI is thus seen to be an essential condition for the synthesis of C-SWNTs. It explains why there must be non-equilibrium conditions to promote the synthesis such as the rapid cooling rate, since it permits, on one hand, the formation of the precursors for the synthesis of C-SWNTs, and on the other hand, the formation of a supersaturated liquid layer below the eutectic temperature by insuring a rapid segregation process. It is necessary to have a catalyst NP with a nanometer-scale liquid layer supersaturated in carbon, in order to favour the BMI. We believe that the particular structure of the catalyst NP, especially the nanometer-scale liquid layer, is responsible for the nucleation of a bundle of C-SWNTs. With a thicker liquid layer, one could imagine the appearance of a new pattern, which could permit the nucleation of a C-MWNT.

The BMI model has thus allowed us to clarify certain aspects of the growth of C-SWNTs by coupling hydrodynamic instabilities with chemical reactions far from equilibrium conditions. The process can thus be seen as non-equilibrium crystal growth (a reaction–convection system) since it results from the spontaneous generation of a dissipative structure, the Bénard–Marangoni cells, in a medium far from equilibrium. In future work, it will be interesting to study in more detail the BMI growth mechanism and also to try to extend it to other filamentary structures (nanowires and nanotubes of other materials) since they could be also the result of a convection cell flow crystallization.

Acknowledgments

The authors would like to thank Pr. J.-P. Dodelet, Pr. B. Terreault and J. Duquette for their helpful discussions and also Guy Lebrun for drawings.

References

[1] Baughman RH, Zakhidov AA, de Heer WA. Carbon nanotubes-the route toward applications. Science 2001;297:787–92.
[2] Eletskii AV. Carbon nanotubes. Uspekhi 1997;40(9):899–924.
[3] Kratschmer W, Lamb LD, Fostiropoulos K, Huffman DR. Solid C60: a new form of carbon. Nature 1990;347:354–8.
[4] Journet C, Maser WK, Bernier P, Loiseau A, Lamy de la Chapelle M, Lefrant S, et al. Large-scale production of single-walled carbon nanotubes by the electric-arc technique. Nature 1997;388:756–8.
[5] Guo T, Nikolaev P, Thess A, Colbert DT, Smalley RE. Catalytic growth of single-walled nanotubes by laser vaporization. Chem Phys Lett 1995;243:49–54.
[6] Thess A, Lee R, Nikolaev P, Dai H, Petit P, Robert J, et al. Crystalline ropes of metallic carbon nanotubes. Science 1996;273:483–7.
[7] Alvarez L, Guillard T, Sauvajol JL, Flamand G, Laplaze D. Growth mechanisms and diameter evolution of single wall carbon nanotubes. Chem Phys Lett 2001;342:7–14.
[8] Flamant G, Ferriere A, Laplaze D, Monty C. Solar processing of materials: opportunities and new frontiers. Solar Energy 1999;66:117–32.
[9] Nikolaev P, Bronikowski MJ, Bradley RK, Rohmund F, Colbert DT, Smith KA, et al. Gas-phase catalytic growth of single-walled carbon nanotubes from carbon monoxide. Chem Phys Lett 1999;313:91–7.
[10] Smiljanic O, Stansfield BL, Dodelet J-P, Serventi A, Désilets S. Gas-phase synthesis of swnt by an atmospheric pressure plasma jet. Chem Phys Lett 2002;356:189–93.
[11] Gavillet J, Loiseau A, Ducastelle F, Thair S, Bernier P, Stéphan O, et al. Microscopic mechanisms for the catalyst assisted growth of single-wall carbon nanotubes. Carbon 2002;40:1649–63.
[12] Dijkstra HA. Pattern selection in surface tension driven flow. In: Kulhman HC, Rath H-J, editors. Free surface flows, 391. Wien, New York: Springer: CISM International Centre for Mechanical; 1998. p. 101–44.
[13] Guyon E, Hulin J-P, Petit L. Hydrodynamique physique. Édition du CNRS; 1991. p. 151, 583–8.
[14] Pearson JRA. On convection cells induced by surface tension. J Fluid Mech 1958;4:489–500.
[15] Gorbunov A, Jost O, Pompe W, Graff A. Solid–liquid–solid growth mechanism of single-wall carbon nanotubes. Carbon 2002;40:113–8.
[16] Saito Y. Nanoparticles and filled nanocapsules. Carbon 1995;33:979–88.
[17] Kanzow H, Ding A. Formation mechanism of single-wall carbon nanotubes on liquid-metal particles. Phys Rev B 1999;60:11180–6.
[18] Jost O, Gorbunov AA, Möller J, Pompe W, Liu X, Georgi P, et al. Rate-limiting processes in the formation of single-wall carbon nanotubes: pointing the way to the nanotubes mechanism. J Phys Chem B 2002;106:2875–83.

[19] Gorbunov A, Jost O, Pompe W, Graff A. Role of the catalyst particle size in the synthesis of single-wall carbon nanotubes. Appl Surf Sci 2002;197–198:563–7.
[20] Laplaze D, Alvarez L, Guillard T, Badie JM, Flamant G. Carbon nanotubes: dynamics of synthesis processes. Carbon 2002;40: 1621–34.
[21] Smiljanic O, Larouche F, Sun X, Dodelet J-P, Stansfield BL. Synthesis of c-swnts with a plasma torch: a parametric study. J Nanosci Nanotechnol 2004;4:1005–13.
[22] Puretzsky AA, Schittenhelm H, Fan X, Lance MJ, Allard Jr LF, Geohegan DB. Investigations of single-wall carbon nanotube growth by time-restricted laser vaporization. Phys Rev B 2002;65: 245425-1–5-9.
[23] Krivoruchko OP, Zaikovskii VI. Formation of liquid phase in the carbon–metal system at unusually low temperature. Kinetics Catal 1998;39:561–70.
[24] Krivoruchko OP, Zaikovskii VI. A new phenomenon involving the formation of liquid mobile metal–carbon particles in the low-temperature catalytic graphitisation of amorphous carbon by metallic Fe, Co and Ni. Mendeleev Commun 1998;3:97–100.
[25] Fan X, Buczko R, Puretzsky AA, Geohegan DB, Howe JY, Pantelides ST, et al. Nucleation of single-walled carbon nanotubes. Phys Rev Lett 2003;90:145501-1–1-4.
[26] Lopez MJ, Rubio A, Alonso JA, Qin L-C, Iijima S. Novel polygonized single-wall carbon nanotube bundles. Phys Rev Lett 2001;86:3056–9.
[27] Gavillet J, Thibault J, Stéphan O, Amara H, Loiseau A, Bichara Ch, et al. Nucleation and growth of single-walled nanotubes: the role of metallic catalysts. J Nanosci Nanotechnol 2004;4:346–59.
[28] Nishio M, Seiji A, Nakayama Y. Cooling effect on the growth of carbon nanotubes and optical emission spectroscopy in short-period arc-discharge. Thin Solid Films 2004;464–465:304–7.
[29] Schatz MF, Neitzel GP. Experiments on thermocapillary instabilities. Ann Rev Fluid Mech 2001;33:93–127.
[30] Cartwright JHE, Piro O, Villacampa AI. Pattern formation in solutal convection: vermiculated rolls and isolated cells. Physica A 2002;314:291–8.
[31] Angus HT. Cast iron physical and engineering properties. Butterworths; 1976. p. 123.
[32] Eremenko VN. The role of surface phenomena in metallurgy. Consultants Bureau Enterprises 1963:90.
[33] Baïlon J-P, Dorlot J-M. Des matériaux. Presse Internationale Polytechnique; 2000. p. 204.
[34] Brian PLT. Effect of Gibbs adsorption on Marangoni instability. AIChE 1971;17:765–72.
[35] Hall N. The new chemistry. Cambridge University Press; 2000. p. 440–65.
[36] Kondepudi D, Prigogine I. Modern thermodynamics: from heat engines to dissipative structures. John Wiley & Sons; 1998. p. 427–57.
[37] Velarde MG. Drops, liquid layers and the Marangoni effect. Philos Trans: Math, Phys Eng Sci 1998;356:829–44.
[38] Kataura H, Kumazawa Y, Maniwa Y, Ohtsuka Y, Sen R, Suzuki S, et al. Diameter control of single-walled carbon nanotubes. Carbon 2000;38:1691–8.
[39] Bandow S, Asaka S, Saito Y, Rao AM, Grigorian L, Richter E, et al. Effect of the growth temperature on the diameter distribution and chirality of single-wall carbon nanotubes. Phys Rev Lett 1998;80:3779–82.
[40] Dil'man VV, Kulov NN, Naidenov VI. Onset of instability due to Marangoni effect. Nova Science Publishers Inc.; 1996. p. 57–110.
[41] Mills KC. The effect of interfacial phenomena on materials processing. In: Velarde MG, Zeytounian RKh, editors. Interfacial phenomena and the Marangoni effect, 428. Wien, New York: Springer: CISM International Centre for Mechanical Sciences; 2002. p. 226–83.